ACS APPLIED MATERIALS & INTERFACES

Research Article

www.acsami.org

Quantitative Dispersion Analysis of Inclusions in Polymer Composites

Mostafa Yourdkhani and Pascal Hubert*

Department of Mechanical Engineering, McGill University, 817 Sherbrooke Street West, Montreal, Quebec H3A 3C0, Canada

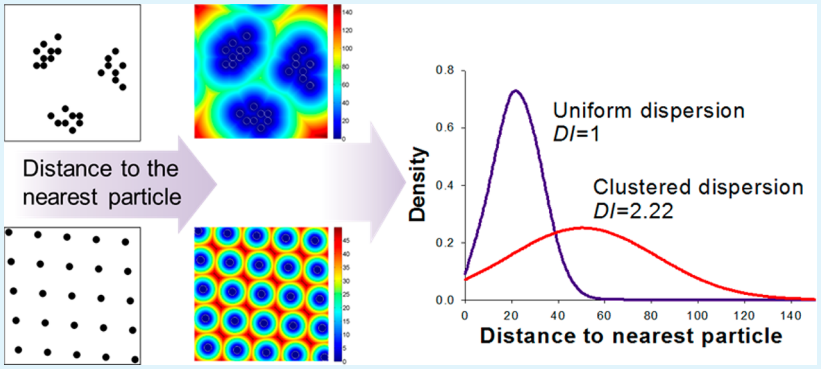

ABSTRACT: The state of dispersion plays an important role on the performance of polymer nanocomposites. Dispersion is usually assessed based on the qualitative evaluation of microscopy micrographs. In this paper, a quantitative algorithm is introduced for analyzing the dispersion of inclusions in polymer composites using image analysis. In a binary image, on-pixels are considered as particle elements while off-pixels stand for matrix elements. To quantify the dispersion, the mean distance value between any matrix elements to their corresponding nearest neighboring particle element is measured. A dispersion index, *DI*, is then defined by comparing the image of interest with the associated uniformly dispersed case. Synthetic models were utilized to examine the sensitivity of the algorithm to various dispersity scenarios such as the effect of particle size, clustering, and cluster distribution. Optical micrographs of carbon nanotube modified epoxy with different states of dispersion were also employed to assess the applicability and functionality of the algorithm to real micrographs.

KEYWORDS: *filler dispersion, nanoparticle, composite, image analysis, dispersion analysis*

1. INTRODUCTION

The state of dispersion is one of the key parameters in the synthesis of carbon nanotube (CNT) modified polymers.[1−4] CNTs are commercially available in the form of entangled bundles; this entanglement is caused by the large van der Waals attraction that exists between individual nanotubes owing to their large specific surface area and aspect ratio.[5−7] As a result, it is necessary to apply a sophisticated method to efficiently separate and disperse CNTs inside the polymer matrix. To exploit the full potential of CNTs in the mechanical reinforcement of polymers, a uniform dispersion with minimum number and size of aggregates is desirable; however, it may not be always possible to reach the full state of dispersion because of the reasons mentioned above.

Various techniques have been used to analyze the dispersion of nanoparticles inside polymers. Kim et al.[8] analyzed the dispersion of CNTs inside epoxy using the results of differential scanning calorimetry (DSC). They assumed that CNTs' dispersion hinders the full cross-linking of epoxy resin resulting in lower heat of reaction. Dispersion was then analyzed based on the degree of cross-linking. This method requires running DSC experiments on all samples, which is costly and time-consuming, and the concept is not generally accurate since low volume fractions of CNTs cannot significantly alter the cross-linking of thermosetting resin. Raman spectroscopy was also used to characterize the dispersion of CNTs in an aqueous solution.[9,10] The intensity of a Raman peak at 267 cm was used as a basis to measure the degree of agglomeration. This method not only requires performing spectroscopy experiments on the samples, but also requires further knowledge and analysis of the results obtained from the spectroscopy measurements.

Apart from these methods, various types of microscopy observations have been widely employed to visually analyze the state of dispersion. Observations are usually made at two levels of hierarchy, that is, microscale and nanoscale. Optical microscopy is employed to visualize the dispersion of CNTs aggregates at the microscale[11,12] while scanning electron microscopy (SEM), transmission electron microscopy (TEM), and atomic force microscopy (AFM) can identify the dispersion of individual nanotubes or CNT bundles at the nanoscale.[13−18]

The information obtained from nanoscale observations is restricted to a very small area of the sample, which may not be

Received: July 31, 2012
Accepted: October 31, 2012
Published: October 31, 2012

   dx.doi.org/10.1021/am301459q | *ACS Appl. Mater. Interfaces* 2013, 5, 35−41

the representative of the overall dispersion. Besides, the time and cost of scanning a large area of the sample with electron microscopy are prohibitive. Optical microscopy on the other hand can provide useful information about the size of aggregates at the microscale. In dispersion analysis, it is always practical to observe the dispersion quality first at the microscale to identify the distribution of aggregates. If the microscale dispersion is acceptable, nanoscale microscopy can then be used to visualize the dispersion of individual nanoparticles in more detail.

The dispersion analysis of images obtained from microscopy techniques are usually performed qualitatively to distinguish between a good and a bad dispersion; however, it is not always easy to visually examine the state of dispersion. Therefore, it is necessary to develop a robust algorithm that can automatically evaluate the state of dispersion. Luo and Koo[19−21] proposed a method to quantify the dispersion of various particles inside a polymer matrix by measuring the free-path spacing between the particle surfaces. A probability density function was then used to define a dispersion quantity parameter. In their method, the effect of particle size, shape, and clustering was not taken into consideration. Glaskova et al.[22,23] used the same approach but measured the particle size to determine the quality of dispersion. Dispersion was recognized to be good if particles of uniform size are dispersed inside the matrix. However, particle distribution is not considered in their method. In another study, Yazdanbakhsh et al.[24,25] defined the concept of "dispersive work", which is the work required to transfer particles to a uniform distribution, to quantify the dispersion of inclusions in composites. Bakshi et al.[26] defined a clustering parameter by measuring the fraction of distances between the centroids of CNTs that are less or equal to five times the CNT diameter. In other studies, the size distribution of filler aggregates has been used as a criterion to analyze the dispersion.[27−29] In a recent study, Li et al.[30] quantified the dispersion based on calculating the probability density function of the kernel density for an image and comparing it with a uniform dispersion.

Although the preceding methods can capture some aspects of particle dispersion, the need still remains for a robust and comprehensive method that can take all aspects into consideration. In this article, a novel algorithm for the quantitative dispersion analysis of particles in composites is proposed.

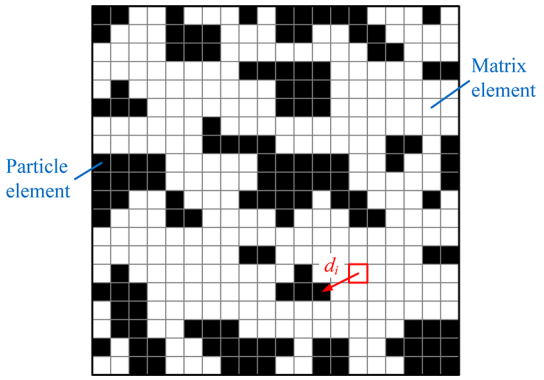

Figure 1. Representative binary image showing pixels of matrix (white) and particle (black) elements. The distance between a matrix element to the nearest neighboring particle element, d_i, is shown.

2. DISPERSION QUANTIFICATION ALGORITHM

The complete dispersion of individual nanoparticles is necessary for exploiting their large surface-to-volume ratio. In a uniform dispersion, each individual particle is distributed evenly throughout the matrix such that the minimum distance between the particles is maximized. Deviation from a uniform dispersion occurs when the particles of different sizes or particle

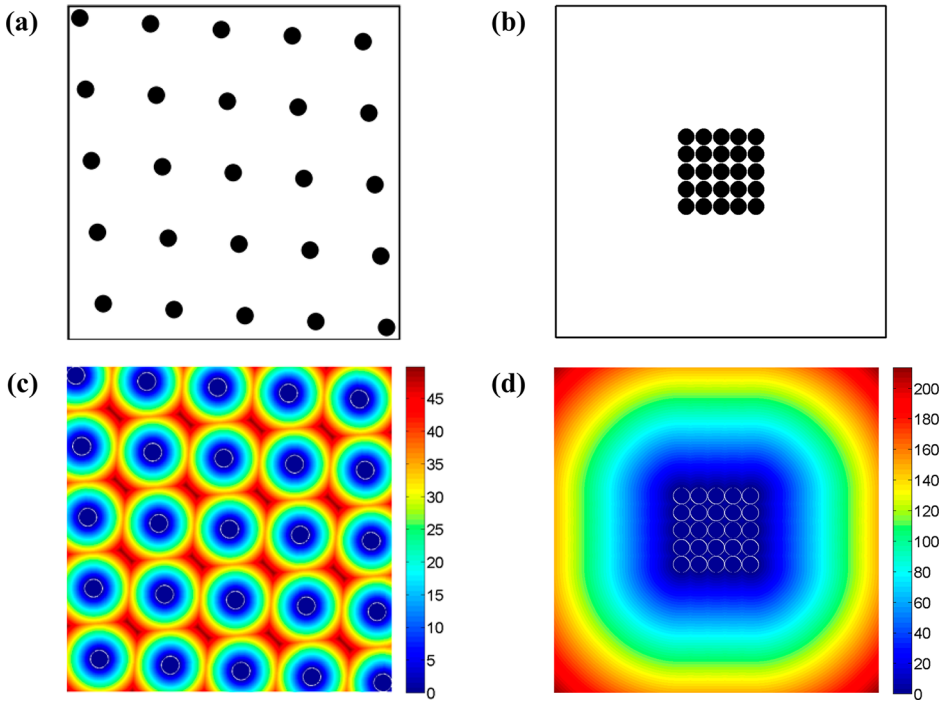

Figure 2. Synthetic model showing the case of (a) ideal uniform dispersion (DI = 1.00); (b) agglomerated dispersion (DI = 4.21). The corresponding nearest neighbor distance distribution is illustrated in (c) for the image in (a), and in (d) for the image in (b). Colorbar depicts the distribution of distances in the units of number of elements.

dx.doi.org/10.1021/am301459q | ACS Appl. Mater. Interfaces 2013, 5, 35−41

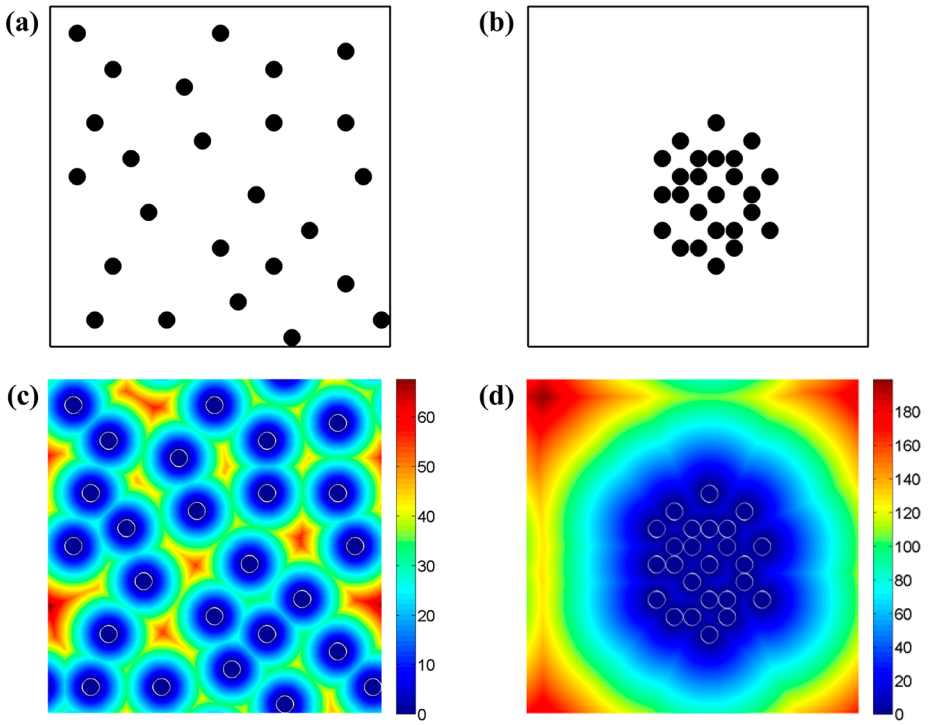

Figure 3. Synthetic model showing the case of (a) random dispersion (DI = 1.07); (b) clustered dispersion (DI = 3.39). The corresponding nearest neighbor distance distribution is illustrated in (c) for the image in (a), and in (d) for the image in (b). Colorbar depicts the distribution of distances in the units of number of elements.

clustering are observed. To distinguish between different states of dispersion, a new algorithm is proposed here. It is assumed here that there is enough contrast between particles and background in the dispersion image. In this algorithm, any pixel in a binary image is referred as an "element". A white pixel represents a "matrix element" while a black pixel denotes a "particle element" (see Figure 1). It is noteworthy to mention that the existing algorithms in the literature are based on the distance between particle elements whereas the proposed algorithm relies on the distance between the matrix elements and particle elements.

For a given dispersion image, the distance between a matrix element to the nearest neighboring particle element, d_i, is computed (Figure 1). The mean value of all nearest neighbor distances, μ, can be obtained by

$$\mu = \frac{\sum_{i=1}^{N_m} d_i}{N_m} \quad (1)$$

where N_m is the number of matrix elements. The value of μ represents how the matrix elements are positioned around the particle elements. It should be mentioned that for the elements close to the edge of the micrograph, the calculated distances are restricted to the neighboring elements that exist in the micrograph; however, to include the information from the neighboring regions in the analysis, periodic boundary conditions are assumed here along different directions. As a result, the nearest neighbor distances are calculated for a larger representative area of the sample.

The proposed algorithm was implemented in MATLAB (The MathWorks, Natick, MA, U.S.A.). First, each image was converted into a binary image whose information was stored into an array. Using an array operation, the nearest neighboring particle element to each matrix element was found and the corresponding distance was computed. Then, the mean value of all the computed distances was obtained. Let us consider two extreme cases: an ideal uniform dispersion and an agglomerated dispersion (Figures 2a and b). In each case, 25 identical spherical particles with an areal fraction of 5% in a 400 × 400 elements matrix domain are considered. The distribution of nearest neighbor distances for the two cases is shown in Figures 2c and d, respectively. These figures are plotted also in MATLAB based on the values of nearest neighbor distances obtained from the array operations as explained in the previous part. The color assigned to each element displays how far (in units of number of elements) that element is to its nearest particle element; for instance, an element with a red color has the highest distance to its nearest particle element compared with the other elements in the figure. Besides, the colorbar on each image indicates the value of the nearest neighbor distance associated with each color.

For the uniform dispersion (Figure 2a), all particles are completely surrounded by the matrix and are distributed uniformly within the image resulting in an even distribution of nearest neighbor distances with small mean value. However, for the agglomerated dispersion (Figure 2b), the minimum fraction of the matrix is influenced by the particles. In this case, the value of nearest neighbor distance increases as the matrix elements get farther from the agglomerated region.

To compare the dispersion of different systems with different areal fractions, the mean nearest neighbor distance introduced in eq 1 is normalized with respect to the corresponding ideal dispersed image.

To find the ideal uniformly dispersed case for a given image, it is assumed that any aggregates or bundles of particles that exist in the image are broken down to the separate individual particles. If individual particles cannot be recognized, which is the case in optical micrographs obtained from the dispersion of nanoparticles, individual particle element is considered instead. Once the individual particles are determined, they are positioned in a uniformly

dx.doi.org/10.1021/am301459q | ACS Appl. Mater. Interfaces 2013, 5, 35−41

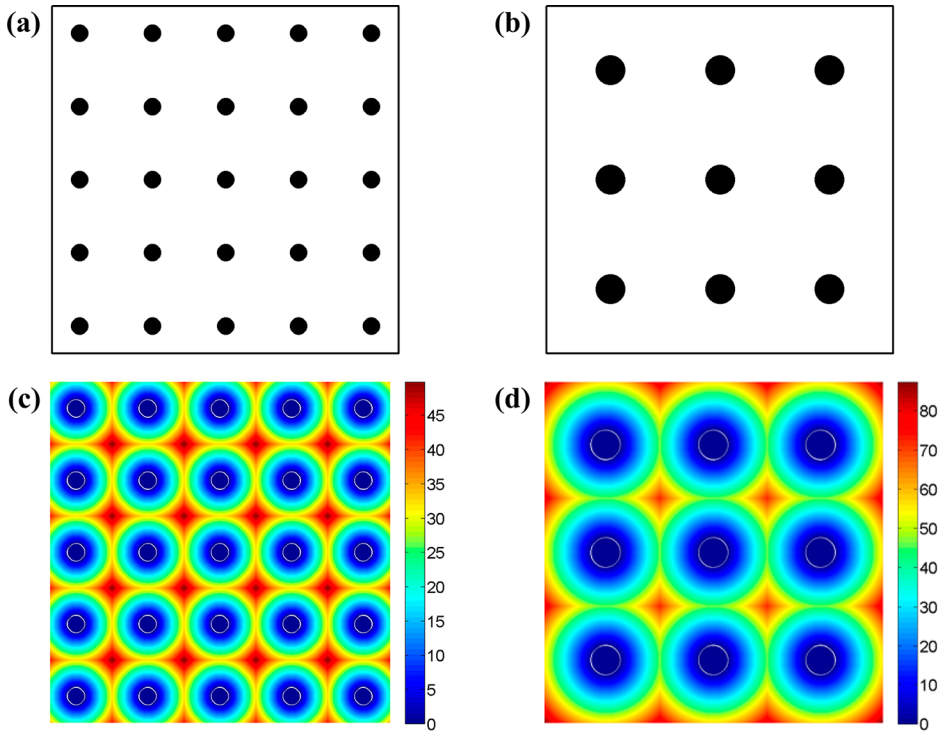

Figure 4. Synthetic model showing the case of (a) dispersion of small particles (DI = 1.04); (b) dispersion of large particles (DI = 1.59). The corresponding nearest neighbor distance distribution is illustrated in (c) for the image in (a), and in (d) for the image in (b). Colorbar depicts the distribution of distances in the units of number of elements.

dispersed arrangement via the maximin algorithm assuming a space-filling and noncollapsing dispersion (Figure 2a).[31,32]

Finally, the corresponding mean nearest neighbor distance for the ideal uniformly dispersed image, μ_u, is calculated as

$$\mu_u = \frac{\sum_{i=1}^{N_m} d_{u,i}}{N_m} \tag{2}$$

where $d_{u,i}$ is the distance between each matrix element to the nearest neighboring particle element. μ_u represents the minimum feasible value of the mean nearest neighbor distance that one can obtain for the given image of dispersion. A dispersion index, DI, is then defined as

$$DI = \frac{\mu}{\mu_u} \tag{3}$$

DI indicates how far the dispersion is from the case of ideal uniform dispersion. Therefore, DI = 1 for a uniformly dispersed system whereas its value increases as the dispersion gets worse. In the following sections, synthetic and real images are used to validate the proposed algorithm with different dispersity scenarios.

3. APPLICATION OF THE PROPOSED ALGORITHM ON SYNTHETIC MODELS

To assess the sensitivity of the proposed algorithm to different dispersity scenarios, different synthetic models are produced that will be explained in detail in the following subsections. Similar to the images used in Figure 2, each model image consists of 25 identical spherical particles with an areal fraction of 5% in a 400 × 400 elements matrix domain unless otherwise specified.

3.1. Effect of Particle Clustering. Clustering is mainly related to the distribution of particles within the matrix. If particles are homogenously distributed, more regions of matrix are influenced with the particles resulting in a good reinforcing behavior. However, if clustering takes place, particles concentrate in certain regions leaving the rest of the matrix uncovered. In Figure 3a, a relatively well-dispersed model is compared with a clustered dispersion in Figure 3b. The corresponding plots of nearest neighbor distance distribution are shown in Figures 3c and d. When the particles form a cluster, they do not allow the matrix to fully exfoliate them and as a result, most of the matrix regions are left uncovered with particles. Hence, a small portion of the matrix elements are close to the clustered particles and the rest are located at farther distances. In this situation, variation in the values of the nearest neighbor distances is significantly large with a large value of DI indicating a poor state of dispersion.

3.2. Effect of Particle Size. Ideal dispersion favors breaking the aggregates down to the individual particles. If aggregates or bundles of particles are present in a system, the surface-to-volume ratio is reduced and less effective reinforcement is achieved. It is of great interest to disperse particles individually to cover as much of the matrix regions as possible. Particle size becomes an issue when analyzing the dispersion of nanoparticles in optical micrographs. Obviously, particles that are observed in the optical micrographs are the aggregates of nanoparticles rather than individual nanoparticles. A good microscale dispersion is achieved if particles (aggregates) with small size are formed. To investigate the effect of particle size, the 25 identical particles in Figure 4a are rearranged to form nine larger particles in Figure 4b while maintaining the areal fraction fixed. Figures 4c and d present the nearest neighbor distance distribution for the cases in Figures 4a and b, respectively. As particles enlarge because of aggregation from Figure 4a to Figure 4b, the fraction of the matrix influenced with particles decreases and large distance values are observed accordingly. As a result, the mean distance

dx.doi.org/10.1021/am301459q | ACS Appl. Mater. Interfaces 2013, 5, 35−41

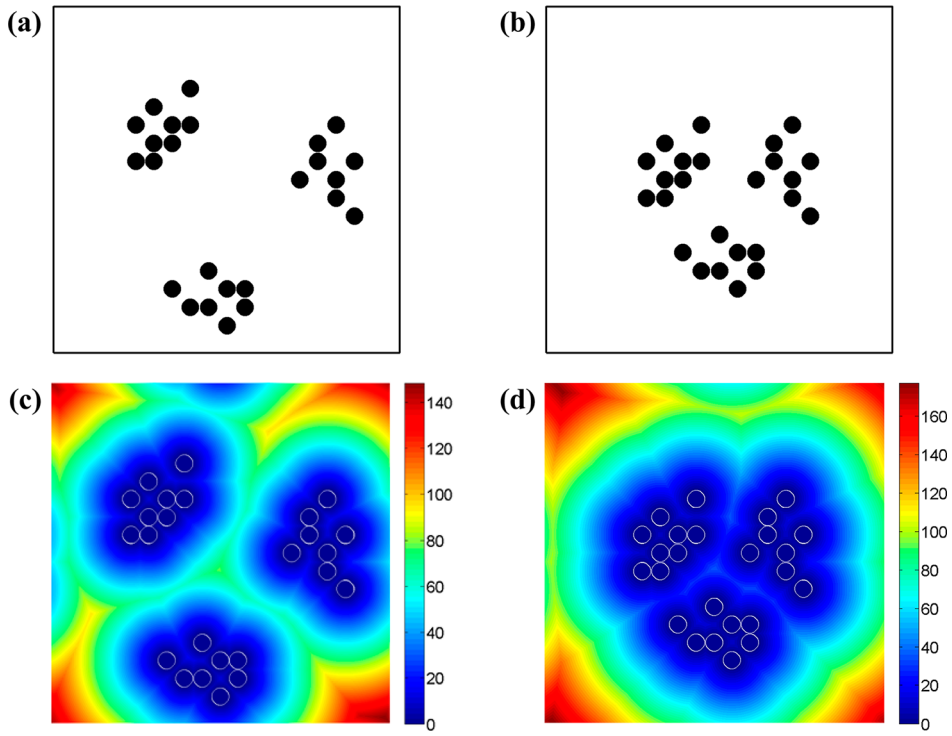

Figure 5. Synthetic model showing the case of (a) better distribution of clusters (*DI* = 2.22); (b) worse distribution of clusters (*DI* = 2.75). The corresponding nearest neighbor distance distribution is illustrated in (c) for the image in (a), and in (d) for the image in (b). Colorbar depicts the distribution of distances in the units of number of elements.

value and correspondingly *DI* increases as the particle size increases indicating a worse state of dispersion.

3.3. Effect of Cluster Distribution. Clusters formation is not limited to a specific region and can occur at different places of the matrix. If clusters are distributed into different regions of the matrix relatively far from each other (Figure 5a), the matrix can fill the regions between the clusters and thereby smaller matrix rich regions are found. However, if clusters are formed relatively close to each other (Figure 5b), particles are concentrated locally where the chance of reinforcing the remaining part of the matrix becomes low. As it can be seen from Figure 5, *DI* is capable of distinguishing properly between different cases of clusters distribution.

3.4. Comparison of Synthetic Models. To elucidate more and compare the state of dispersion for the cases shown in Figures 2−5, the probability density function (PDF) for the distribution of the nearest neighbor distances is plotted in Figure 6. Besides, the corresponding value of *DI* for each case is displayed in the legend. A good dispersion is recognized by small mean and standard deviation values in the PDF curve. For instance, the PDF of the ideal uniform dispersion (the case in Figure 2a) is found to have the smallest mean value, highest peak, and smallest standard deviation. As dispersion deviates from the uniform state, the curves are shifted toward larger mean values with larger standard deviation and lower peak height.

As a summary, the synthetic models used here confirm the sensitivity of the current algorithm to different visually assessable states of dispersion.

4. APPLICATION OF THE PROPOSED ALGORITHM ON REAL MICROGRAPHS

In addition to the synthetic images, real experimental micrographs are employed to explore the validity of the proposed

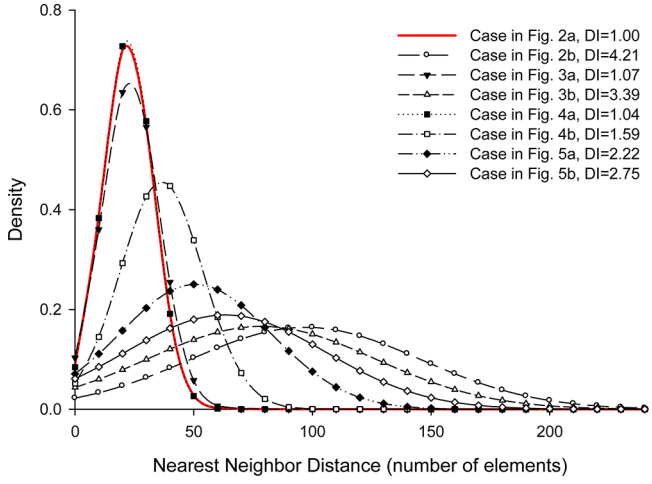

Figure 6. PDF of distribution of nearest neighbor distances for the cases presented in Figures 2−5. The value of *DI* is also shown in the legend.

algorithm. Multiwall carbon nanotubes (MWNT) were used as filler particles inside Epon 828 epoxy resin. The MWNTs, which were supplied by Baytubes, were synthesized based on chemical vapor deposition (CVD) and had a mean outer diameter of 13−16 nm with an aspect ratio of around 100 to 500. Isophorone Diamine (IPD) was used as the curing agent with the resin-to-hardener ratio of 100:23. MWNTs were mixed with epoxy resin using a high shear mixer, and samples with MWNT concentration of 0.3 wt.% were prepared. To investigate the stability of dispersion during the resin cure cycle, in situ hot stage microscopy was applied. A droplet of sample was placed on a glass substrate inside a Linkam THMS 600 hot

dx.doi.org/10.1021/am301459q | *ACS Appl. Mater. Interfaces* 2013, 5, 35−41

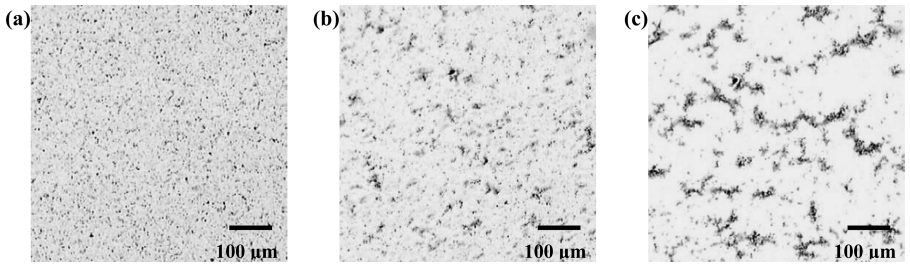

Figure 7. Optical micrographs of MWNT/epoxy samples illustrating the evolution of dispersion at (a) 25 °C; (b) 60 °C; (c) 120 °C. *DI* was calculated as 1.51 in (a), 2.37 in (b), and 5.55 in (c).

stage. The hot stage was then placed under an Olympus BX50 transmission optical microscope through which the micrographs were acquired at 250× magnification. A heating rate of 3 °C/min was applied to the sample via the hot stage. Figure 7 illustrates three images that were captured at different temperatures to show the evolution of dispersion during the resin cure. As the temperature rises, resin viscosity drops, and the mobility of nanotubes increases resulting in reagglomeration of CNTs with a poor state of dispersion.[29] The algorithm proposed in this study is used to quantitatively assess the state of dispersion during the resin cure. It is worth mentioning that since optical micrographs display microscale dispersion, aggregates of CNTs are considered as particle elements in the dispersion analysis. As a result, dispersion indices (*DI*) of 1.51, 2.37, and 5.55 were respectively calculated for Figures 7a, b and c, which indicate the degradation of dispersion with temperature. The results of dispersion quantification are in a good agreement with the visual assessment of dispersion degree confirming the practicality and robustness of the proposed algorithm.

5. CONCLUSIONS

A novel algorithm was developed to quantify the dispersion of inclusions in polymer composites using image analysis. According to the proposed algorithm, any given image is divided into matrix and particle elements based on which the distance between each matrix element to the nearest particle element is calculated. In a good dispersion, the nearest neighboring distances are evenly distributed throughout the matrix with the smallest possible mean value. However, as the dispersion degrades, the nearest neighbor distances vary from small values in regions close to particles to large values in regions far from particles. Therefore, the mean distance value increases accordingly implying the degradation of dispersion. A dispersion index, *DI*, is then defined by comparing the mean value of the nearest neighbor distances for the given image with that of an ideal uniformly dispersed case. $DI = 1$ for the case of ideal uniform dispersion while it increases as the dispersion degrades.

To assess the sensitivity of the current algorithm to various dispersity scenarios, synthetic models and real micrographs were used. The effect of particle size, clustering, and cluster distribution was examined to verify the robustness and applicability of the proposed algorithm. The algorithm was also applied on optical micrographs of CNT-modified epoxy to confirm the visual assessment of dispersion evolution during the resin cure. As a result, this algorithm can be applied to quantitatively analyze the state of dispersion of particles inside different matrices at any scale.

AUTHOR INFORMATION

Corresponding Author

*Tel: (514) 398-6303. Fax: (514) 398-7365. E-mail: pascal.hubert@mcgill.ca.

Notes

The authors declare no competing financial interest.

REFERENCES

(1) Ma, P. C.; Mo, S. Y.; Tang, B. Z.; Kim, J. K. *Carbon* **2010**, *48*, 1824−1834.
(2) Li, J.; Ma, P. C.; Chow, W. S.; To, C. K.; Tang, B. Z.; Kim, J. K. *Adv. Funct. Mater.* **2007**, *17*, 3207−3215.
(3) Rahmat, M.; Hubert, P. *Compos. Sci. Technol.* **2011**, *72*, 72−84.
(4) Martone, A.; Formicola, C.; Giordano, M.; Zarrelli, M. *Compos. Sci. Technol.* **2010**, *70*, 1154−1160.
(5) Schadler, L.; Giannaris, S.; Ajayan, P. *Appl. Phys. Lett.* **1998**, *73*, 3842−3844.
(6) Darsono, N.; Yoon, D. H.; Kim, J. *Appl. Surf. Sci.* **2008**, *254*, 3412−3419.
(7) Rastogi, R.; Kaushal, R.; Tripathi, S. K.; Sharma, A. L.; Kaur, I.; Bharadwaj, L. M. *J. Colloid Interface Sci.* **2008**, *328*, 421−428.
(8) Kim, S. H.; Lee, W. I.; Park, J. M. *Carbon* **2009**, *47*, 2699−2703.
(9) Yoon, D.; Choi, J. B.; Han, C. S.; Kim, Y. J.; Baik, S. *Carbon* **2008**, *46*, 1530−1534.
(10) Heller, D. A.; Barone, P. W.; Swanson, J. P.; Mayrhofer, R. M.; Strano, M. S. *J. Phys. Chem. B* **2004**, *108*, 6905−6909.
(11) Chakraborty, A. K.; Plyhm, T.; Barbezat, M.; Necola, A.; Terrasi, G. P. *J. Nanopart. Res.* **2011**, *13*, 6493−6506.
(12) Vaisman, L.; Wagner, H. D.; Marom, G. *Adv. Colloid Interface Sci.* **2006**, *128*, 37−46.
(13) Gommes, C.; Blacher, S.; Masenelli-Varlot, K.; Bossuot, C.; McRae, E.; Fonseca, A.; Nagy, J. B.; Pirard, J. P. *Carbon* **2003**, *41*, 2561−2572.
(14) Fan, Z. H.; Hsiao, K. T.; Advani, S. G. *Carbon* **2004**, *42*, 871−876.
(15) Pegel, S.; Potschke, P.; Villmow, T.; Stoyan, D.; Heinrich, G. *Polymer* **2009**, *50*, 2123−2132.
(16) Rahmat, M.; Das, K.; Hubert, P. *ACS Appl. Mater. Interfaces* **2011**, *3*, 3425−3431.
(17) Rahmat, M.; Ghiasi, H.; Hubert, P. *Nanoscale* **2012**, *4*, 157−166.
(18) Hubert, P.; Ashrafi, B.; Adhikari, K.; Meredith, J.; Vengallatore, S.; Guan, J. W.; Simard, B. *Compos. Sci. Technol.* **2009**, *69*, 2274−2280.
(19) Luo, Z. P.; Koo, J. H. *J. Microsc. (Oxford, U. K.)* **2007**, *225*, 118−125.
(20) Luo, Z. P.; Koo, J. H. *Polymer* **2008**, *49*, 1841−1852.
(21) Luo, Z. P.; Koo, J. H. *Mater. Lett.* **2008**, *62*, 3493−3496.
(22) Glaskova, T.; Zarrelli, M.; Borisova, A.; Timchenko, K.; Aniskevich, A.; Giordano, M. *Compos. Sci. Technol.* **2011**, *71*, 1543−1549.
(23) Glaskova, T.; Zarrelli, M.; Aniskevich, A.; Giordano, M.; Trinkler, L.; Berzina, B. *Compos. Sci. Technol.* **2012**, *72*, 477−481.
(24) Yazdanbakhsh, A.; Grasley, Z.; Tyson, B.; Abu Al-Rub, R. K. *Composites, Part A* **2011**, *42*, 75−83.

(25) Grasley, Z. C.; Yazdanbakhsh, A. *Composites, Part A* **2011**, *42*, 2043−2050.
(26) Bakshi, S. R.; Batista, R. G.; Agarwal, A. *Composites, Part A* **2009**, *40*, 1311−1318.
(27) Le, H. H.; Ilisch, S.; Radusch, H. J. *Polymer* **2009**, *50*, 2294−2303.
(28) Ryszkowska, J. *Mater. Charact.* **2009**, *60*, 1127−1132.
(29) Mirjalili, V.; Yourdkhani, M.; Hubert, P. *Nanotechnology* **2012**, *23*, 315701−315708.
(30) Li, Z.; Gao, Y.; Moon, K. S.; Yao, Y.; Tannenbaum, A.; Wong, C. *Polymer* **2012**, *53*, 1571−1580.
(31) Rennen, G.; Husslage, B.; Van Dam, E.; Den Hertog, D. *Struct. Multidiscip. Optim.* **2010**, *41*, 371−395.
(32) van Dam, E. R.; Husslage, B.; den Hertog, D.; Melissen, H. *Oper. Res.* **2007**, *55*, 158−169.